

## Tolerogenic nanoparticles targeting B and T lymphocytes delay autoimmune arthritis in K/BxN mice.

Amrita Srivastava,<sup>a</sup> Britni M. Arlian,<sup>a</sup> Lijuan Pang,<sup>a</sup> Takashi K. Kishimoto<sup>c</sup> and James C. Paulson<sup>a,b\*</sup>

<sup>a</sup>Department of Molecular Medicine, The Scripps Research Institute, La Jolla, CA 92037 United States.

<sup>b</sup>Department of Immunology and Microbiology, The Scripps Research Institute, La Jolla, CA 92037 United States.

<sup>c</sup>Selecta Biosciences Inc., Watertown, MA 02472 United States.

---

\* Correspondence: Dr. James C. Paulson, Professor and Co-Chair, Department of Molecular Medicine, Affiliated with Department of Immunology & Microbiology, 10550 North Torrey Pines Road, MB-202, La Jolla, CA 92037, Phone : 858-784-9634, FAX: 858-784-9690, Email: [jpaulson@scripps.edu](mailto:jpaulson@scripps.edu)

## Abstract

**Objective:** This study aims to examine the therapeutic potential of combined treatment with B cell targeted STALs and T cell targeted PLGA-R nanoparticles in treating K/BxN mice that develop spontaneous autoimmune arthritis to the self-antigen glucose-6-phosphate-isomerase (GPI).

**Methods:** Siglec-engaging tolerance-inducing antigenic liposomes (STALs) that display both an antigen (Ag) and glycan ligands of the inhibitory co-receptor CD22 (CD22L) were prepared by thin film hydration method. Rapamycin encapsulated PLGA nanoparticles (PLGA-R) were prepared by the oil in water single emulsion method. The K/BxN arthritis mice were treated intravenously with GPI-STALs and PLGA-R nanoparticles prophylactically and therapeutically. Disease progression was monitored by paw thickness measurements and GPI-specific IgG titers were determined by serum ELISAs. Changes in cartilage and synovium were evaluated by histological analysis.

**Results:** Co-administration of STALs together with PLGA-R to naïve mice induced more robust tolerance to multiple antigen challenges than either nanoparticle alone. Repeated dosing was beneficial as co-administration of 5 doses of GPI-STALs and PLGA-R prophylactically delayed disease onset until 11 weeks, and in some cases indefinitely. Therapeutic treatment of K/BxN mice with GPI-STALs and PLGA-R after disease symptoms are apparent showed prevention and, in some cases, even reversal of disease. In addition, histological examination of treated K/BxN mice showed normal cartilage and synovium and the absence of infiltrating immune cells into the joint space as compared to untreated mice.

**Conclusion:** Together these data show synergy between B cell-tolerizing STALs and T cell-tolerizing PLGA-R and the potential to induce tolerance in early stage autoimmune disease.

## Keywords

Nanoparticles, Immune tolerance, K/BxN, Arthritis, Siglec.

## INTRODUCTION

Undesired immune responses are responsible for numerous human maladies including autoimmune diseases<sup>1,2</sup>, allergies<sup>3</sup>, transplantation rejection<sup>4,5</sup>, and production of inhibitory antibodies to biotherapeutic medicines<sup>6</sup>. Existing treatments for these conditions are not antigen-specific and therefore lead to broad immune suppression with numerous adverse effects<sup>7</sup>. Thus, to suppress undesired immune activation, antigen-specific tolerance approaches are needed that provide immune tolerance to the antigen of interest while leaving the rest of the immune system intact.

Various approaches have been used to induce antigen-specific immune tolerance by targeting B or T cells<sup>8-11</sup>. Each B cell is specific to a single antigen, and when stimulated differentiate into antibody-secreting plasma cells. Thus, a direct approach to induce antigen-specific humoral tolerance targets antigen-reactive B cells<sup>12,13</sup>. B cells express a set of B cell receptor (BCR) inhibitory coreceptors<sup>14</sup>, including CD22 and Siglec-G (Siglec-10 in humans), members of the sialic acid-binding immunoglobulin-like lectin (Siglec) family that recognize sialic acid-containing glycans of glycoproteins and glycolipids<sup>15-17</sup>. Co-presentation of antigen with ligands of CD22 or Siglec-G on liposomal nanoparticles results in recruitment of the Sigelects to the immunological synapse formed when a B cell receptor (BCR) engages the antigen<sup>18-20</sup>. This engagement leads to a potent apoptotic signal resulting in elimination of antigen-reactive B cells, leaving the rest of the B cell repertoire unaffected, and induction of B cell tolerance due to depletion of the antigen-specific B cells<sup>21</sup>. The utility of Siglec tolerizing antigenic liposomes (STALs) has been successfully demonstrated in several models of disease, one involving the generation of inhibitory antibodies to FVIII in hemophilia mice<sup>18</sup>, another involving tolerization of animals to allergen sensitization in a peanut antigen anaphylaxis model<sup>22,23</sup>, and a third involving apoptosis of autoantigen-specific memory B cells from RA patients<sup>24</sup>. STALs are particularly effective in naïve animals since there is minimal activation of CD4+ T cells that are required for B cells to differentiate into cells that produce high affinity antibodies of the IgG class, and are less suitable for inducing tolerance in animals with an ongoing immune response with antigen specific CD4+ T helper or T memory cells.

An alternative for inducing antigen-specific tolerance is through direct targeting of the T cell arm of the immune response. Currently available to allergic patients is allergen immunotherapy (AIT) where gradually increasing doses of antigen are administered by injection or orally to patients over several years to build up tolerance. While AIT has been helpful in desensitizing patients to antigen, there is limited long lasting desensitization when treatment ends<sup>23,25,26</sup>. Another approach aimed at treating ongoing immune responses involves targeting of antigen experienced T cells with peptide-MHC bound nanoparticles to induce T regulatory cells (Tregs), but this technology requires knowledge of the precise peptide antigen recognized by the T cells<sup>27,28</sup>. Other approaches seek to program T cells through antigen-presenting cells (APCs) presented with antigen coupled to syngeneic cells<sup>29,30</sup>, or synthetic particles carrying antigens and/or immune-modulators<sup>31-38</sup>. The general strategy is to create tolerogenic APCs that secrete cytokines to induce antigen-specific anergy/deletion of T cells, or reprogram them to Tregs<sup>10,11,27</sup>.

A particularly attractive option currently in clinical development involves administering of antigen with poly(lactic co-glycolic acid) (PLGA) particles containing the immunomodulator rapamycin. Initially, Maldonado *et al.* showed that PLGA nanoparticles encapsulated with both antigen and the immunomodulatory drug rapamycin could induce robust tolerance to a variety of antigens in naïve animals<sup>32</sup>. Subsequently, it was shown that PLGA nanoparticles with rapamycin (PLGA-R) co-injected with soluble antigen produced equally robust tolerance<sup>33,34,37-39</sup>. Mechanistic studies support the idea that the non-targeted rapamycin-PLGA particles efficiently deliver the drug to

APCs to create a tolerogenic cytokine environment, which in turn induces Tregs that prevent activation of T helper cells needed by B cells to produce inhibitory antibodies<sup>32-34 39</sup>.

Because the tolerogenic nanoparticle technologies targeting the B cell and T cell arms of the immune system operate by different mechanisms, we reasoned that they might be synergistic, providing more robust tolerance than either alone. Initial attempts to incorporate rapamycin into the lipid bilayer of STALs showed improved tolerance induction in naïve mice, but were limited by the dose of rapamycin that could be achieved and had insignificant impact on tolerance induction in previously sensitized mice<sup>40</sup>. Here we have compared the two tolerogenic nanoparticle platforms alone or in combination under various conditions of antigen presentation and tested them for preventing inflammatory disease in the antigen-specific K/BxN arthritis model. Administering STALs and PLGA-R in combination significantly suppressed antibody production to liposomal-antigen over either nanoparticle alone. In K/BxN mice that develop autoimmune rheumatoid arthritis (RA) dependent on production of antibodies to the self-protein, glucose-6-phosphate isomerase (GPI)<sup>41-43</sup>, neither GPI-STALs or PLGA-R alone had significant impact on the onset of disease. When administered together weekly for up to 5 weeks, the onset of disease was delayed, and some mice remained disease free for up to 150 days. Some benefit could also be achieved by delaying treatment until ankle swelling was apparent. The results suggest that combining these B and T cell targeted tolerance strategies hold promise for suppressing unwanted immune reactions.

## **MATERIALS AND METHODS**

Detailed experimental procedures are described in supplementary materials and methods (see online supplementary file).

## **RESULTS AND DISCUSSION**

### **Nanoparticle synthesis and characterization**

Unless otherwise noted, STALs and PLGA-R nanoparticles were prepared as previously described with few modifications<sup>18,32</sup>. For incorporation into liposomes (LP), the mouse CD22 ligand (CD22L) was coupled to pegylated-lipid (Figure 1A) and the protein antigen (Ag) was also coupled to lipid as described<sup>18</sup>. Schematic illustrations of STALs (Ag-LP-CD22L) and PLGA-R nanoparticles are shown in Figure 1B.

STALs with ovalbumin (OVA) as antigen (OVA-STALs; OVA-LP-CD22L) and biodegradable PLGA-R nanoparticles were characterized by dynamic light scattering (DLS) and transmission electron microscopy (TEM) (Figure 1C-D). The hydrodynamic diameter of OVA-LP-CD22L and PLGA-R was found to be  $156\pm 32$  and  $182\pm 31$ , respectively, as measured by DLS. TEM characterization confirmed that both OVA-LP-CD22L and biodegradable PLGA-R showed uniform spherical morphology.

### **STALs and PLGA-R synergize to produce enhanced tolerance**

Since STALs are formulated with protein antigen, STALs and PLGA-R were tested alone and in combination for their ability to suppress antibody production against liposomal ovalbumin (OVA-LP or OVA-LP-CD22L) in C57BL/6J mice. The concentration of OVA (0.1 mol %) and CD22 ligand (1.5 mol %) used in the STALs was selected based on previously optimized formulations<sup>18 40</sup>. PLGA-R nanoparticles contained 50-100  $\mu\text{g}$  of rapamycin as earlier studies indicated this as an optimal dose for inducing tolerance<sup>37 38</sup>. Similar formulations of STALs and PLGA nanoparticles have been reported to have serum half-lives in mouse blood of 11 and 16 hours, respectively<sup>44 45</sup>. Mice were treated (i.v.) once (day 0), or twice (days 0 and 14) with OVA-LP, OVA-STALs (OVA-LP-CD22L) or OVA-LP and PLGA-R, followed by challenge i.p. 14 and 35 days later with OVA/Alum and free OVA (fOVA), respectively. With one treatment, analysis of anti-OVA serum titers showed

that treatment with OVA-STALs or PLGA-R alone or together significantly reduced serum titers of OVA relative to mice treated with OVA-LP. Moreover, OVA-LP-CD22L and PLGA-R together further reduced anti-OVA IgG1 titers relative to mice treated with STALs or OVA-LP + PLGA-R alone, demonstrating synergy between the two tolerogenic nanoparticle systems (Figure 2A).

With two treatments at 0 and 14 days, greater tolerance to OVA challenge was evident with the combined treatment with OVA-LP-CD22L + PLGA-R showing significantly greater suppression than either nanoparticle alone (Figure 2B). Notably, while OVA-LP + PLGA-R induced weak suppression of anti-OVA production, two treatments with fOVA + PLGA-R induced strong tolerance equivalent to OVA-STALs + PLGA-R (see online supplementary figure S1). Thus, we suggest that PLGA-R is more effective at inducing tolerance with monovalent antigen than the multivalent antigen exemplified by OVA-LP.

Since the strategy for combining STALs and PLGA-R envisioned the induction of CD4<sup>+</sup> antigen specific regulatory T cells that would synergize with STALs for suppression of B cell activation<sup>32</sup>, we investigated production of Tregs in naïve mice. OVA specific CD4<sup>+</sup> T cells (OTII cells) were adoptively transferred into naïve mice and the next day mice were treated with OVA-STALs (OVA-LP-CD22L) alone or with one or two doses of OVA-STALs + PLGA-R. On day 28 post-treatment, the number of Foxp3<sup>+</sup>CD25<sup>+</sup>OTII T cells in spleen were evaluated (see online supplementary figure S2). While no Treg induction was observed with OVA-STALs alone, Tregs were induced when OVA-STALs were administered together with PLGA-R nanoparticles.

### **Treatment of K/BxN arthritis mice with tolerogenic nanoparticles delays onset of disease symptoms**

To evaluate the potential for the combined STALs + PLGA-R nanoparticle treatments to modulate autoimmune disease, we chose the K/BxN autoimmune rheumatoid arthritis (RA) model<sup>41-43</sup>. The K/BxN arthritis model recapitulates many histological features of human rheumatoid arthritis, including cartilage and bone destruction, leukocyte invasion, synovitis, and pannus formation. This is an ideal model since it is caused by development of autoimmune antibodies to the self-antigen glucose-6-phosphate isomerase (GPI), and both B and T cells are required for disease onset and pathology. K/BxN mice express the TCR transgene KRN and MHC class II molecule A<sup>g7</sup>, spontaneously produce GPI reactive antibodies, and develop chronic RA symptoms as they age<sup>41-43</sup>. Since the relevant antigen for the K/BxN model is GPI, an abundant self-antigen made by every cell, K/BxN mice are not “naïve” to the antigen, even at birth. All mice develop symptoms of RA and begin to exhibit ankle swelling at day 25-30 after weaning, allowing treatments to begin prior to disease onset. For these experiments, GPI-STALs were prepared in a manner analogous to OVA-STALs<sup>18</sup>.

K/BxN mice were injected i.v. with 1, 2, or 5 doses of nanoparticles every 6-7 days, starting at 21-25 days of age, and monitored for disease progression by measuring front and hind paw thickness three times per week (Figure 3A). Mice were considered to be at the study endpoint when one or more joint(s) measured 4 mm. GPI-STALs (GPI-LP-CD22L) and PLGA-R nanoparticles administered separately in two doses failed to alter disease progression since the median survival of mice (percentage of mice without disease) treated with either nanoparticles was not significantly different from untreated mice (37, 39, and 36 days for untreated, GPI-LP-CD22L-treated, and PLGA-R-treated mice, respectively; Figure 3B). However, when GPI-LP-CD22L and PLGA-R were co-delivered to K/BxN mice using the 1, 2, or 5-time dosing scheme (Figure 3C), disease progression was significantly delayed, demonstrating synergy of combining the two nanoparticles. The delay in disease progression was dose-dependent, as the median survival of mice without disease was 47.5, 56, and 80 days for mice treated with 1, 2, or 5 doses of GPI-LP-CD22L + PLGA-R, respectively. Astonishingly, none of the mice treated 5 times with GPI-LP-CD22L + PLGA-R had

disease by 70 days of age, twenty days after dosing ended, and a few mice remained disease free to the end of the 150 day study.

Although we assumed that mice had abundant endogenous free antigen, we also investigated treatment of mice with PLGA-R with exogenous free soluble GPI (fGPI) or GPI liposomes (GPI-LP) without CD22L. Accordingly, mice were injected with fGPI (25  $\mu$ g) + PLGA-R or GPI-LP + PLGA-R using the 5-dose injection scheme. Co-injection of PLGA-R with exogenous fGPI or GPI-LP dramatically delayed onset of disease (Figure 3D). However, in both of the antigen + PLGA-R groups, 25-40% of the mice developed disease before the end of dosing at 50 days. This delay in onset of disease can be seen in mean disease severity for each group, measured as the sum of ankle thickness for all four paws over time (Figure 3E). Thus, while antigen + PLGA-R (Figure 3D) was clearly better than PLGA-R alone (Figure 3B), treatment with GPI-STALs + PLGA-R provided a further significant delay (Figure 3D, 3E), and was the only treatment that delayed the onset of disease for all mice during treatment and for nearly 20 days after treatment ended.

To assess disease progression histologically, ankle sections from untreated wild-type C57BL/6J mice (Figure 4A-D) and K/BxN mice at 55 days that were untreated (Figure 4E-H) or treated with five weekly doses of GPI-LP-CD22L+PLGA-R (Figure 4I-L) were stained with Safranin O/Fast Green to assess protection of the joints under the different treatment conditions. Normal cartilage characterized by maintenance of Safo staining, chondrocyte numbers, and the bone matrix was seen in the treated K/BxN mice and untreated wild-type mice. In addition, the synovium in treated K/BxN mice and untreated wild-type mice was healthy, without the severe inflammation and infiltration of immune cells into the joint space that was evident in the untreated K/BxN mice. Finally, minimal bone resorption at the cartilage/bone margin was seen in the treated K/BxN mice and untreated wild-type mice compared to severe bone resorption in the untreated K/BxN mice. Together these histochemical data suggest treatment with the nanoparticles can prevent damage to the cartilage, bone, and joint space.

We also assessed the serum anti-GPI IgG titers from treated and untreated K/BxN mice by ELISA (Figure 4 M-N). While untreated K/BxN mice developed high anti-GPI titers, mice treated with GPI-STALs + PLGA-R for 5 consecutive weeks, maintained very low anti-GPI titers, providing direct evidence that the treatments suppressed antibody production to GPI.

### **Therapeutic treatment of K/BxN arthritis mice delays progression of disease**

Although K/BxN mice are born with the propensity to develop autoimmune joint disease mediated by antibodies to GPI, we considered that once the disease symptoms had started, progression may be resistant to treatment with GPI-STALs + PLGA-R. However, motivated by the delayed onset of arthritis when treatment was initiated soon after weaning, we sought to test for efficacy when the first treatment was initiated after disease onset when at least one paw was swollen to a thickness of 2.8-3.05 mm. Mice were then either left untreated or given 5 weekly doses of GPI-LP-CD22L + PLGA-R containing either 50 or 100  $\mu$ g of rapamycin (Figure 5A). For this study, we used total joint thickness, the sum of the thickness of all four paws, as a measure of disease severity. For untreated mice ( $n = 17$ ), disease progressed rapidly with all mice achieving a score of >12 mm by day 40. Of the mice administered with GPI-LP-CD22L + PLGA-R containing 50  $\mu$ g of rapamycin per treatment (Figure 5B, *middle panel*,  $n = 17$ ), all but one mouse showed a delay in achieving a score of 12, and 9 of 17 mice showed a more significant delay. Remarkably, 3 mice either had no progression, or progressed and then reversed disease severity. Moreover, 2 out of 5 mice administered with GPI-LP-CD22L + PLGA-R containing 100  $\mu$ g of rapamycin per treatment showed no progression (Figure 5B, *right panel*). These results suggest that the combination of GPI-STALs + PLGA-R is able to significantly delay or prevent disease in a prophylactic modality and even reverse the disease progression in a therapeutic treatment modality. We further analyzed the anti-GPI titers for the mice left untreated versus mice treated with GPI-STALs + PLGA-R on days 30-35 and 50-55 (Figure 5C). While anti-GPI titers for the mice left untreated or treated with 50  $\mu$ g/dose increased

significantly over this period, there was no significant increase in titers for mice treated with 100 µg/dose rapamycin.

## CONCLUSIONS

We found that co-administration of B cell-targeted STALs and T cell-targeted PLGA-R act synergistically to induce more robust antigen-specific tolerance compared to either nanoparticle alone. Repeated dosing was beneficial, which was particularly evident in the delay of disease onset and progression in the K/BxN arthritis model. Co-administration of 5 doses of GPI-LP-CD22L and PLGA-R prior to display of arthritis delayed disease onset until 11 weeks, with some mice remaining disease-free for the duration of the 150-day study. Therapeutic treatment of K/BxN mice with GPI-LP-CD22L and PLGA-R, after disease onset, when anti-GPI IgG1 titers had increased, showed prevention and, in some cases, even reversal of disease. Together results suggest the potential of the combined treatments to treat early stage autoimmune diseases, particularly in view of the fact that STALs have been demonstrated to suppress antigen specific human memory B cells from rheumatoid arthritis patients<sup>24</sup>, and that B cell depleting therapy such as rituximab (anti-CD20) is therapeutically effective in a rheumatoid arthritis setting<sup>46 47</sup>.

**Acknowledgments** We thank the following individuals at The Scripps Research Institute: Kevin Worrell for synthesis of the mCD22 ligand, Merissa Olmer for the histochemical staining protocol, Dr. Theresa Fassel for microscopy, and Anna Tran-Crie for help with preparation of the manuscript.

**Author Contributions** A.S., J.C.P. and T.K.K. conceived of the project. A.S., J.C.P. and B.M.A. designed the experiments and analyzed data. A.S. designed, developed and characterized the nanoparticles. Experiments were performed primarily by A.S. with help of B.M.A. L.P. conducted one confirmatory study. A.S. and J.C.P. wrote the manuscript with contributions from B.M.A. All authors participated in editing the manuscript.

**Funding** This work was funded in part by NIH grants R01AI099141 & R01AI050143.

**Competing interests** None declared.

**Ethics approval** All experimental procedures involving mice in this work were approved by the Institutional Animal Care and Use Committee of The Scripps Research Institute (La Jolla, CA).

**Data availability statement** Data are available on reasonable request. All data relevant to the study are included in the article or uploaded as online supplementary information.

## ORCID iD

James C. Paulson: <http://orcid.org/0000-0003-4589-5322>

## REFERENCES

1. Naparstek Y, Plotz PH. The role of autoantibodies in autoimmune disease. *Annu Rev Immunol* 1993;11:79-104.
2. Lleo A, Invernizzi P, Gao B, et al. Definition of human autoimmunity-autoantibodies versus autoimmune disease. *Autoimmun Rev* 2010;9:A259-66.
3. Gould HJ, Sutton BJ. IgE in allergy and asthma today. *Nat Rev Immunol* 2008;8:205-17.
4. Kwun J, Bulut P, Kim E, et al. The role of B cells in solid organ transplantation. *Semin Immunol* 2012;24:96-108.
5. Clatworthy MR. Targeting B cells and antibody in transplantation. *Am J Transplant* 2011;11:1359-67.
6. Singh SK. Impact of product-related factors on immunogenicity of biotherapeutics. *J Pharm Sci* 2011;100:354-87.
7. Vassilopoulos D, Calabrese LH. Risks of immunosuppressive therapies including biologic agents in patients with rheumatic diseases and co-existing chronic viral infections. *Curr Opin Rheumatol* 2007;19:619-25.
8. Miller SD, Turley DM, Podojil JR. Antigen-specific tolerance strategies for the prevention and treatment of autoimmune disease. *Nat Rev Immunol* 2007;7:665-77.
9. Sabatos-Peyton CA, Verhagen J, Wraith DC. Antigen-specific immunotherapy of autoimmune and allergic diseases. *Curr Opin Immunol* 2010;22:609-15.
10. Pearson RM, Casey LM, Hughes KR, et al. In vivo reprogramming of immune cells: Technologies for induction of antigen-specific tolerance. *Adv Drug Deliv Rev* 2017;114:240-55.
11. Kishimoto TK, Maldonado RA. Nanoparticles for the Induction of Antigen-Specific Immunological Tolerance. *Front Immunol* 2018;9:230.
12. Manjarrez-Orduno N, Quach TD, Sanz I. B cells and immunological tolerance. *J Invest Dermatol* 2009;129:278-88.
13. Barr TA, Gray M, Gray D. B cells: programmers of CD4 T cell responses. *Infect Disord Drug Targets* 2012;12:222-31.
14. Tsubata T. Role of inhibitory BCR co-receptors in immunity. *Infect Disord Drug Targets* 2012;12:181-90.
15. Crocker PR, Paulson JC, Varki A. Siglecs and their roles in the immune system. *Nat Rev Immunol* 2007;7:255-66.
16. Jellusova J, Nitschke L. Regulation of B cell functions by the sialic acid-binding receptors siglec-G and CD22. *Front Immunol* 2011;2:96.
17. Macauley MS, Crocker PR, Paulson JC. Siglec-mediated regulation of immune cell function in disease. *Nat Rev Immunol* 2014;14:653-66.
18. Macauley MS, Pfrengle F, Rademacher C, et al. Antigenic liposomes displaying CD22 ligands induce antigen-specific B cell apoptosis. *J Clin Invest* 2013;123:3074-83.
19. Pfrengle F, Macauley MS, Kawasaki N, et al. Copresentation of antigen and ligands of Siglec-G induces B cell tolerance independent of CD22. *J Immunol* 2013;191:1724-31.
20. Macauley MS, Paulson JC. Siglecs induce tolerance to cell surface antigens by BIM-dependent deletion of the antigen-reactive B cells. *J Immunol* 2014;193:4312-21.
21. Duong BH, Tian H, Ota T, et al. Decoration of T-independent antigen with ligands for CD22 and Siglec-G can suppress immunity and induce B cell tolerance in vivo. *J Exp Med* 2010;207:173-87.



22. Orgel KA, Duan S, Wright BL, et al. Exploiting CD22 on antigen-specific B cells to prevent allergy to the major peanut allergen Ara h 2. *J Allergy Clin Immunol* 2017;139:366-69 e2.
23. Burks AW, Calderon MA, Casale T, et al. Update on allergy immunotherapy: American Academy of Allergy, Asthma & Immunology/European Academy of Allergy and Clinical Immunology/PRACTALL consensus report. *J Allergy Clin Immunol* 2013;131:1288-96 e3.
24. Bednar KJ, Nycholat CM, Rao TS, et al. Exploiting CD22 To Selectively Tolerize Autoantibody Producing B-Cells in Rheumatoid Arthritis. *ACS Chem Biol* 2019;14:644-54.
25. Investigators PGoC, Vickery BP, Vereda A, et al. AR101 Oral Immunotherapy for Peanut Allergy. *N Engl J Med* 2018;379:1991-2001.
26. MacGinnitie AJ, Rachid R, Gragg H, et al. Omalizumab facilitates rapid oral desensitization for peanut allergy. *J Allergy Clin Immunol* 2017;139:873-81 e8.
27. Irvine DJ, Swartz MA, Szeto GL. Engineering synthetic vaccines using cues from natural immunity. *Nat Mater* 2013;12:978-90.
28. Tsai S, Shameli A, Yamanouchi J, et al. Reversal of autoimmunity by boosting memory-like autoregulatory T cells. *Immunity* 2010;32:568-80.
29. Getts DR, Turley DM, Smith CE, et al. Tolerance induced by apoptotic antigen-coupled leukocytes is induced by PD-L1+ and IL-10-producing splenic macrophages and maintained by T regulatory cells. *J Immunol* 2011;187:2405-17.
30. Grimm AJ, Kontos S, Diaceri G, et al. Memory of tolerance and induction of regulatory T cells by erythrocyte-targeted antigens. *Sci Rep* 2015;5:15907.
31. Getts DR, Martin AJ, McCarthy DP, et al. Microparticles bearing encephalitogenic peptides induce T-cell tolerance and ameliorate experimental autoimmune encephalomyelitis. *Nat Biotechnol* 2012;30:1217-24.
32. Maldonado RA, LaMothe RA, Ferrari JD, et al. Polymeric synthetic nanoparticles for the induction of antigen-specific immunological tolerance. *Proc Natl Acad Sci U S A* 2015;112:E156-65.
33. LaMothe RA, Kolte PN, Vo T, et al. Tolerogenic Nanoparticles Induce Antigen-Specific Regulatory T Cells and Provide Therapeutic Efficacy and Transferrable Tolerance against Experimental Autoimmune Encephalomyelitis. *Front Immunol* 2018;9:281.
34. Mazor R, King EM, Onda M, et al. Tolerogenic nanoparticles restore the antitumor activity of recombinant immunotoxins by mitigating immunogenicity. *Proc Natl Acad Sci U S A* 2018;115:E733-E42.
35. Hlavaty KA, Luo X, Shea LD, et al. Cellular and molecular targeting for nanotherapeutics in transplantation tolerance. *Clin Immunol* 2015;160:14-23.
36. Hunter Z, McCarthy DP, Yap WT, et al. A biodegradable nanoparticle platform for the induction of antigen-specific immune tolerance for treatment of autoimmune disease. *ACS Nano* 2014;8:2148-60.
37. Zhang AH, Rossi RJ, Yoon J, et al. Tolerogenic nanoparticles to induce immunologic tolerance: Prevention and reversal of FVIII inhibitor formation. *Cell Immunol* 2016;301:74-81.
38. Kishimoto TK, Ferrari JD, LaMothe RA, et al. Improving the efficacy and safety of biologic drugs with tolerogenic nanoparticles. *Nat Nanotechnol* 2016;11:890-99.
39. Lim HH, Yi H, Kishimoto TK, et al. A pilot study on using rapamycin-carrying synthetic vaccine particles (SVP) in conjunction with enzyme replacement therapy to induce immune tolerance in Pompe disease. *Mol Genet Metab Rep* 2017;13:18-22.

40. Pang L, Macauley MS, Arlian BM, et al. Encapsulating an Immunosuppressant Enhances Tolerance Induction by Siglec-Engaging Tolerogenic Liposomes. *ChemBioChem* 2017;18:1226-33.
41. Monach PA, Mathis D, Benoist C. The K/BxN arthritis model. *Curr Protoc Immunol* 2008;Chapter 15:Unit 15 22.
42. Ditzel HJ. The K/BxN mouse: a model of human inflammatory arthritis. *Trends Mol Med* 2004;10:40-5.
43. Monach P, Hattori K, Huang H, et al. The K/BxN mouse model of inflammatory arthritis: theory and practice. *Methods Mol Med* 2007;136:269-82.
44. Chen WC, Completo GC, Sigal DS, et al. In vivo targeting of B-cell lymphoma with glycan ligands of CD22. *Blood* 2010;115:4778-86.
45. Rafiei P, Haddadi A. Docetaxel-loaded PLGA and PLGA-PEG nanoparticles for intravenous application: pharmacokinetics and biodistribution profile. *Int J Nanomedicine* 2017;12:935-47.
46. Finckh A, Ciurea A, Brulhart L, et al. B cell depletion may be more effective than switching to an alternative anti-tumor necrosis factor agent in rheumatoid arthritis patients with inadequate response to anti-tumor necrosis factor agents. *Arthritis Rheum* 2007;56:1417-23.
47. Brulhart L, Ciurea A, Finckh A, et al. Efficacy of B cell depletion in patients with rheumatoid arthritis refractory to anti-tumour necrosis factor alpha agents: an open-label observational study. *Ann Rheum Dis* 2006;65:1255-7.

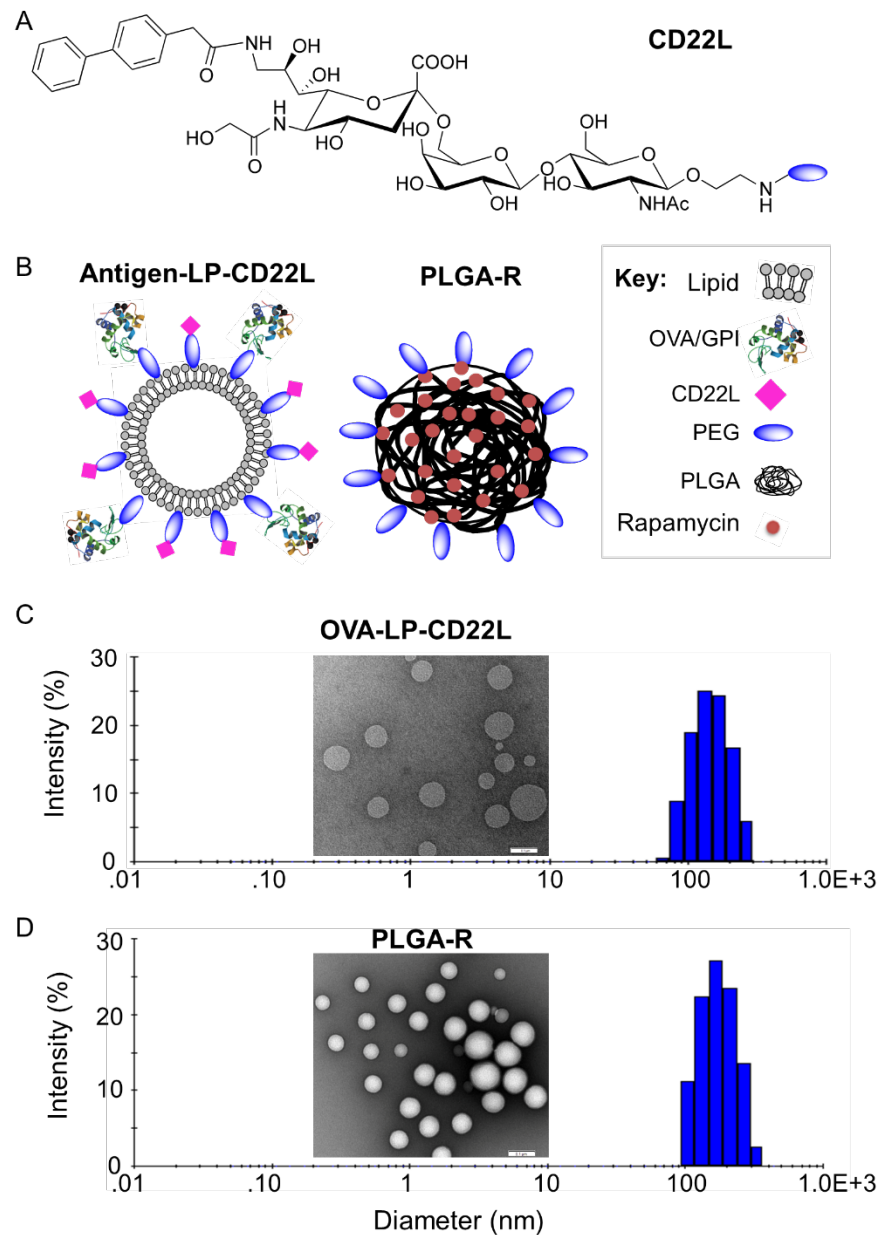


**Figure 1.** Nanoparticle formulation and characterizations. **(A)** Chemical structure of the murine CD22 ligand linked to PEG. **(B)** Schematic illustration of targeted OVA/GPI-STALs (OVA/GPI-LP-CD22L) and PLGA rapamycin (PLGA-R) nanoparticles. **(C-D)** Representative transmission electron microscopic images of OVA-LP-CD22L (inset **C**) and PLGA-R (inset **D**), and hydrodynamic size distribution of OVA-LP-CD22L ( $156\pm32$ ; plot **C**) and PLGA-R ( $182\pm31$ ; plot **D**) as determined by dynamic light scattering.

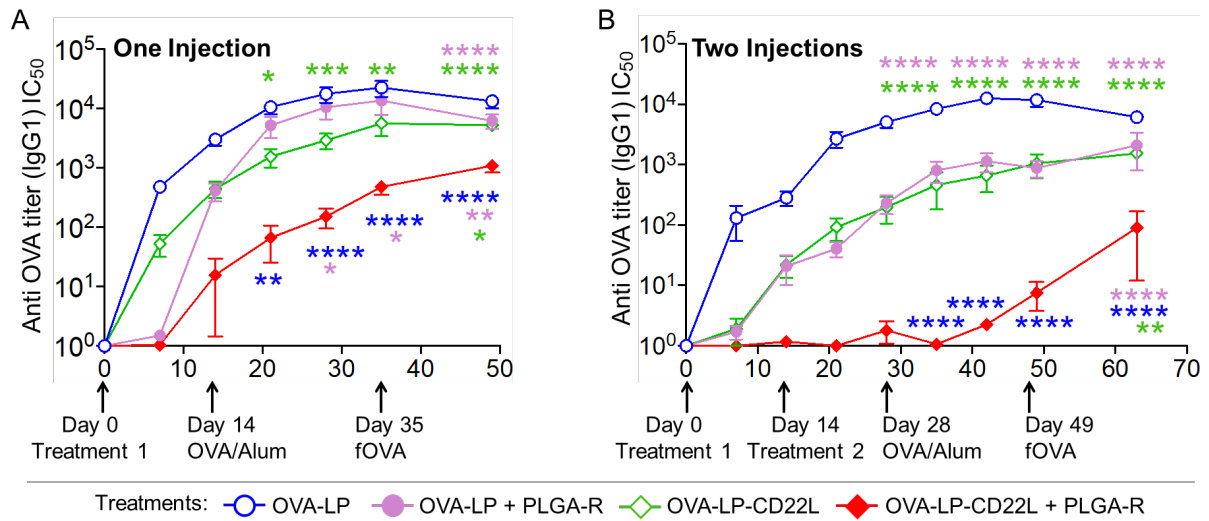


**Figure 2.** Co-delivery of OVA-STALs (OVA-LP-CD22L) and PLGA-R nanoparticles induce greater tolerance to liposomal OVA than either nanoparticle alone. **(A)** C57BL/6J mice ( $n = 16$ ) were immunized on day 0 with the indicated nanoparticle treatments i.v. and then challenged i.p. with OVA/Alum on day 14 and fOVA on day 35. Data were pooled from three independent experiments. **(B)** C57BL/6J mice ( $n = 5$ ) were immunized on days 0 and 14 with the indicated nanoparticle treatments i.v. and then challenged i.p. with OVA/Alum on day 28 and fOVA on day 49 and results are representative of two independent experiments. PLGA-R nanoparticles contained 100  $\mu\text{g}$  of rapamycin<sup>38</sup>. Mice were bled weekly after the treatment, and IgG1 titers were assessed for OVA. Data were normalized by dividing the titers by naive mean and are shown here. All data represent the mean  $\pm$  SEM. All statistical analyses were performed on raw data using two-way ANOVA with Tukey's post-test (\*\*\*\*  $P \leq 0.0001$ ; \*\*\*  $P \leq 0.001$ ; \*\*  $P \leq 0.01$ ; \*  $P \leq 0.05$ ).

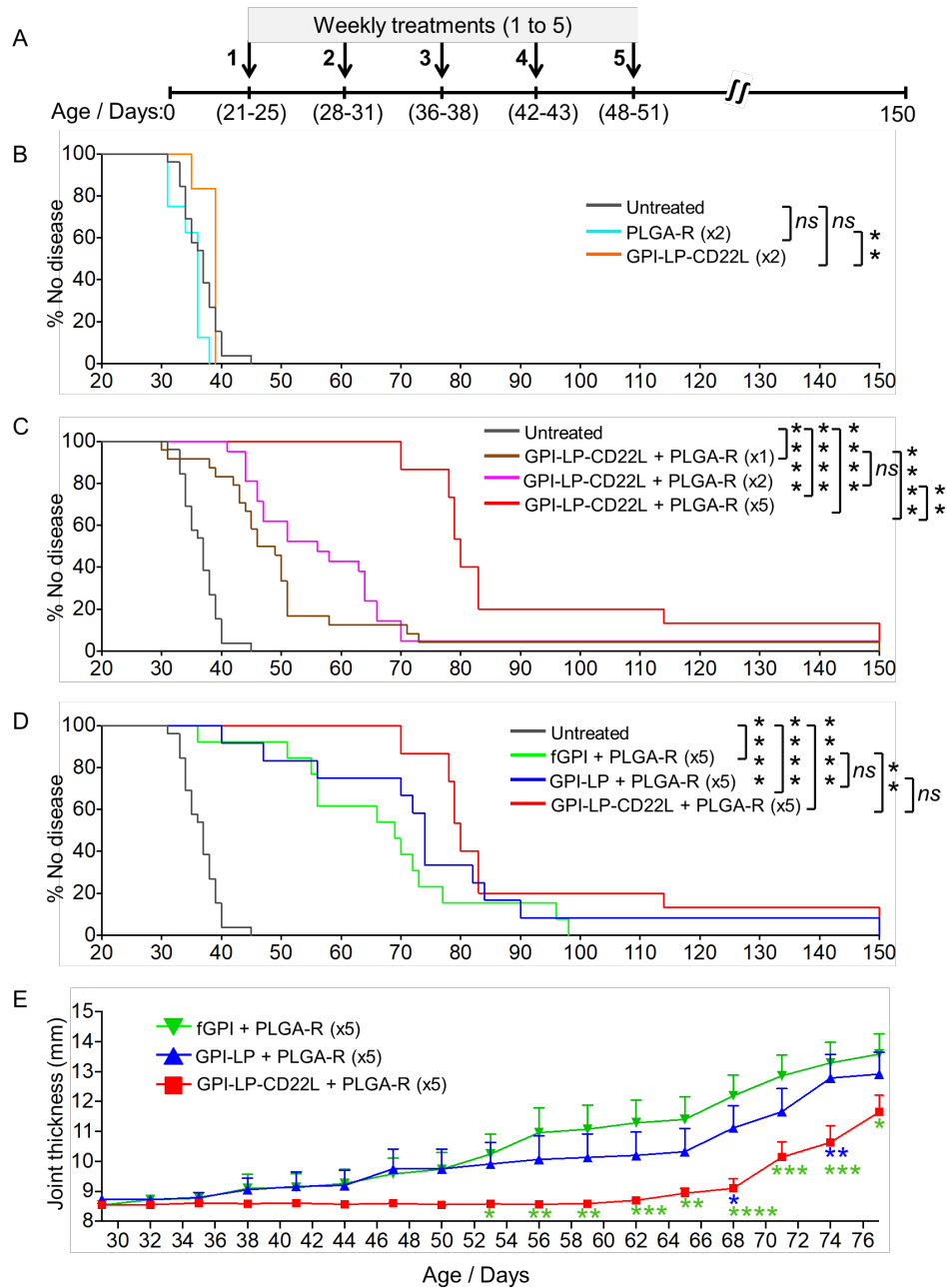


**Figure 3.** Administration of nanoparticles to K/BxN mice prior to onset of arthritis delayed disease. **(A)** Strategy for treating K/BxN mice with one, two, or five doses of nanoparticles prophylactically. PLGA-R nanoparticles contained 100  $\mu$ g of rapamycin. **(B-D)** K/BxN mice, 21-25 days of age, were untreated or treated once (x1) or weekly (6-7 days) for 2 (x2) or 5 (x5) consecutive weeks. Joint measurements were performed three times a week, and mice were considered to be at the study endpoint when one or more joint(s) measured 4 mm. Results over time for each group ( $n = 6-26$ ), are shown as percent of mice with no joint swelling over 4 mm. Results are representative of two experiments. To facilitate comparisons, results for untreated mice and GPI-LP-CD22L (GPI-STALs) + PLGA-R are shown in panels **B-D** and **C-D**, respectively. **(E)** Disease severity assessed as total joint thickness for all four paws in treated mice out to 77 days. Statistical analyses were performed using log-rank test in figure **B-D** and by two-way ANOVA with Tukey's post-test in **E** (\*\*\*\*  $P \leq 0.0001$ ; \*\*\*  $P \leq 0.001$ ; \*\*  $P \leq 0.01$ ; \*  $P \leq 0.05$  and ns indicates not significant).

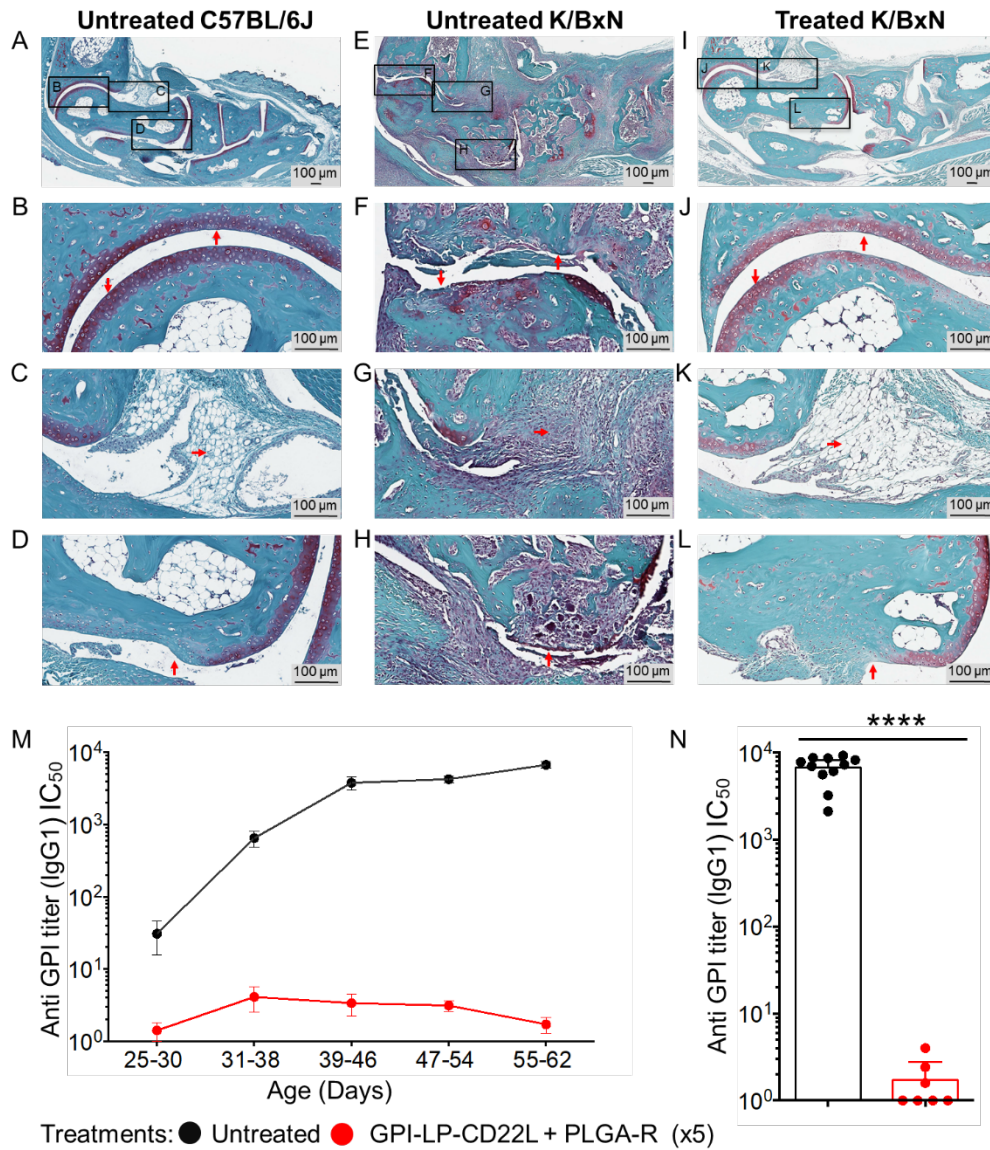


**Figure 4.** Co-administration of GPI-LP-CD22L and PLGA-R protects K/BxN mice from joint damage. Histochemical staining of day 55 paraffin-embedded ankle sections with Safranin O/Fast Green and hematoxylin counterstain reveals gross differences in the joint health of control wild-type mice left untreated (**A**), K/BxN diseased mice left untreated (**E**), and K/BxN diseased mice treated 5 times with GPI-LP-CD22L and PLGA-R (**I**). Higher magnification reveals distinct maintenance of cartilage (**J**), preservation of synovial tissue (**K**), and minimal bone resorption (**L**) in treated K/BxN mice, comparable to healthy controls (**B**, **C**, and **D**), which is in stark contrast to the loss of cartilage (**F**), severe infiltration of immune cells into the synovium (**G**), and severe bone resorption (**H**) seen in diseased K/BxN mice left untreated. Images are representative of two mice for each condition. (**M**) Co-administration of GPI-LP-CD22L and PLGA-R to K/BxN mice suppresses production of anti-GPI serum titers. Anti-GPI IgG titers from untreated K/BxN mice (black,  $n = 11$ ) versus mice co-administered GPI-LP-CD22L and PLGA-R (red,  $n = 7$ ) for 5 consecutive weeks as determined by ELISA. (**N**) Anti-GPI IgG1 titers plotted for days 55-62. All data represent the mean  $\pm$  SEM. Statistical analysis was performed using the Mann-Whitney test (\*\*\*\*  $P \leq 0.0001$ ).

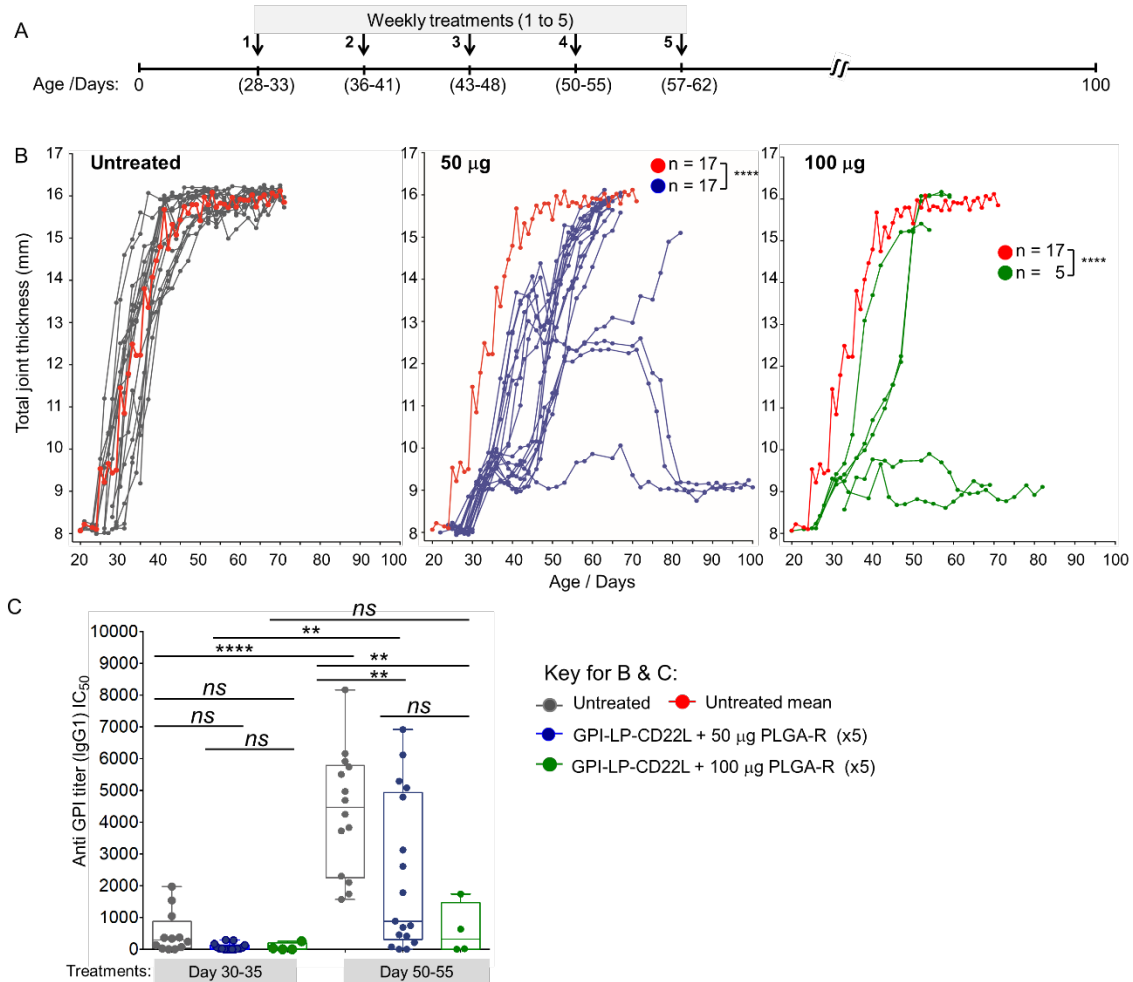


**Figure 5.** Treatment of K/BxN mice after disease onset reduces disease progression. **(A)** K/BxN mice were treated after disease onset measured as >3mm in one or more joints. Mice were either left untreated or treated with 5 weekly injections of both GPI-STALs (GPI-LP-CD22L) and PLGA-R nanoparticles. **(B)** Progression of disease severity measured by total joint thickness for untreated mice (*left panel*) and mice treated with GPI-STALs (GPI-LP-CD22L) and PLGA-R nanoparticles containing either 50 µg (*middle panel*) or 100 µg (*right panel*) of rapamycin. The mean progression for untreated mice (*red curve left panel*) is repeated in the *middle* and *right* panels for comparison. **(C)** Anti-GPI antibody titers from untreated and GPI-STALs + PLGA-R treated K/BxN mice on day 30-35 and day 50-55. Statistical analyses were performed using mixed-effect analysis with a Sidak post-test in **5B** and One-way ANOVA followed by Tukey's test in **5C** (\*\*\*\*  $P \leq 0.0001$ , \*\*  $P \leq 0.01$  and *ns* indicates not significant).

## **Key Messages:**

### **What is already known about this subject?**

K/BxN mice spontaneously produce GPI reactive autoantibodies and develop chronic rheumatoid arthritis symptoms as they age.

Current treatments for unwanted antibody responses are limited, largely relying on immunosuppressive drugs that compromise overall immunity.

### **What does this study add?**

In this report we combine two tolerogenic nanoparticle-based platforms that separately induce tolerance in the B cell (STALs) and T cell (PLGA-R) arms of the immune system in antigen naive animals.

Here we show that these nanoparticles work synergistically to induce profound tolerance to subsequent antigen challenge, and delay onset of disease in the autoimmune K/BxN model of rheumatoid arthritis.

### **How might this impact on clinical practice or future developments?**

Our demonstration that these two nanoparticle platforms work synergistically represents an important advance for developing treatments for autoimmune diseases and undesired immune responses.